Transaction A: Civil Engineering
Vol. 16, No. 4, pp. 297–307

Ductility of High Strength Concrete Heavily Steel Reinforced Members

A.A. Maghsoudi[1,*] and Y. Sharifi[1]

Abstract. *The nature of High Strength Concrete, HSC, is brittle failure and although the behavior of reinforced concrete beams heavily steel reinforced are increased in strength, the ductility, which is important in seismic regions, is in question. In other words, such beams, while consisting of HSC, are more brittle. In this paper, the flexural ductility of such members, with a variation in compressive reinforcement, is investigated. Six heavily reinforced High Strength Concrete, HSC, beams, with different percentages of* ρ *and* ρ'*, were cast and incrementally loaded under bending. During the test, the strain on the concrete middle face and on the tension and compression bars as well as the deflection at different points of the span length were measured up to failure. Based on the results obtained, the curvature, displacement and rotation ductility of the HSC members are more deeply reviewed. A comparison between theoretical and experimental results are also reported here. Generally, it was concluded that for heavily steel reinforced HSC beams, the displacement ductility for singly reinforced beams is too close to the doubly reinforced beams.*

Keywords: *HSC; Displacement; Curvature; Rotation ductility.*

INTRODUCTION

Recent advances in concrete technology have made the use of concrete with strength up to 90 MPa practical. Using High Strength Concrete, HSC, it is possible to reduce the size and weight of reinforced concrete structural members. Concrete with very high compressive strength can result in a less ductile response of structural members. As a flexural element, it is necesssary for beams with high strength concrete to possess good ductility in seismic design and offer beforehand warning to structures by failing. The majority of research work reported is based on under-reinforced HSC members. In other words, the flexural ductility considerations of HSC heavily steel reinforced members need to be further investigated. The results of an investigation carried out on the flexural behavior of HSC heavily reinforced beams, with a variation in compressive reinforcement, are presented.

Six rectangular HSC beams were cast and tested under bending. Load-deflection, moment-curvature and moment-rotation curves were plotted. Three types of ductility factor were employed in this study. A displacement ductility factor, μ_Δ, was defined [1-3] as Δ_u/Δ_y where Δ_u is the displacement at which the compression concrete was crushed and Δ_y is the displacement at which tension steel yields. The curvature ductility factor, μ_φ, was defined [3-5] as φ_u/φ_y where φ_u is the curvature corresponding to Δ_u, and φ_y is the curvature at which tension steel yields. The rotation ductility factor was defined [6] as $\mu_\theta = \theta_u/\theta_y$ where θ_u is the rotation at which the compression concrete was crushed, and θ_y is the rotation at which tension steel yields. All three types of ductility are investigated for the tested HSC heavily steel reinforced beams. A comparison between theoretical and experimental results is also reported.

The exprimental results show [1,7] that it would be more advantageous for the curvature ductility to choose compressive reinforcement while designing members with HSC. However, here it was found that in heavily steel reinforced beams, the displacement ductility for singly reinforced beams is too close to the doubly reinforced beams.

1. *Department of Civil Engineering, Shahid Bahonar University of Kerman, Kerman, P.O. Box 76169-133, Iran.*
*. *Corresponding author. E-mail: maghsoudi.a.a@mail.uk.ac.ir*

Received 22 December 2007; received in revised form 25 September 2008; accepted 7 February 2009

Table 1. Testing program detail of tested beam.

Beam	f'_c (MPa)	d (m)	d' (m)	A_s	A'_s	ρ'/ρ
BC6	73.65	256	40	$4\Phi28$	$2\Phi28$	0.5
B6	71.00	256	-	$4\Phi28$	-	0.0
BC7	66.81	266	40	$4\Phi28 + 2\Phi16$	$3\Phi22 + 2\Phi14$	0.5
B7	70.50	266	-	$4\Phi28 + 2\Phi16$	-	0.0
BC8	77.72	258	42	$2\Phi28 + 6\Phi22$	$2\Phi28 + 2\Phi14 + 1\Phi16$	0.5
B8	71.80	258	-	$2\Phi28 + 6\Phi22$	-	0.0

EXPERIMENTAL PROGRAM

Test Specimens

Six reinforced concrete beams were tested by Sharifi [7] and Mohammad Hasani [8] and the details are reproduced and used. Table 1 presents the detailed testing program. Thus, for the symbols used, B and BC, letter B stands for singly reinforced beams and the letters BC indicate the beams also having compression bars. Three beams were singly reinforced and the other three were doubly reinforced. Shear reinforcements were provided along the beam length except in the constant moment region. The variables were the compressive reinforcement ratio, ρ'.

Materials

Locally available deformed bars with a yield strength of 400 MPa were used as flexural reinforcement. The detailed mix proportions are shown in Table 2. Nowadays to reach high strength concrete, different methods can be followed (i.e., using high amounts of cement in the mix or adopting aggregate types containing high compressive strength such as granite or basalt aggregates. However, here the hight amount of cement with suitable grading was used. All beams and control specimens were cast and cured under similar conditions. A sufficient mixing time was allowed to produce a uniform and homogenous concrete. The concrete strength of each beam was measured by three 100 mm×100 mm×100 mm concrete cube specimens made at the time of casting and kept with the beams during curing. The relationship of cylinder strength (f'_c) and cube strength was assumed as $f'_c = 0.8 f_{cu}$. The beams and the companion concrete specimens were remolded after 24 h and were cured with wet hessian (spraying water twice a day similar to site curing) for 6 days. After that, the specimens were air-cured with a relative humidity of 65-80% and an ambient temperature of 28 ± 3°C until the age of testing. The load was applied statically step-by-step by means of a 1400 kN hydraulic machine.

Test Procedure

The test beams were simply supported and subjected to two-point loads as shown in Figure 1. The beam deflections were measured in four sections using transducers. Strains in the tension and compression steel were measured by electrical strain gauges. Compressive strain at the surface of the concrete at different sections was measured with electrical and mechanical (demec points) strain gauges.

THEORETICAL DUCTILITY

Ductility is the capacity to undergo inelastic deformation and absorb energy. Several forms of ductility are often considered. These include curvature, displacement and rotational ductility. In this research, all three types of ductility are investigated for HSC heavily steel reinforced beams being tested.

Curvature Ductility

Perhaps the most simple and general definition for ductility is curvature ductility. For design, the usual equations for curvatures at yield load (ϕ_y) and at ultimate load (ϕ_u) for under- and balanced-reinforced beams (see Figure 2) are calculated by Maghsoudi [3] and Park and Dai [5]. Generally the calculations can be divided into two following steps:

Table 2. Concrete mix proportion.

Cement (kg/m^3)	Microsilica (kg/m^3)	Coarse Agg. (kg/m^3)	Fine Agg. (kg/m^3)	Super-Plasticizer (kg/m^3)	W/C Ratio
649	55	723	646	11	0.32

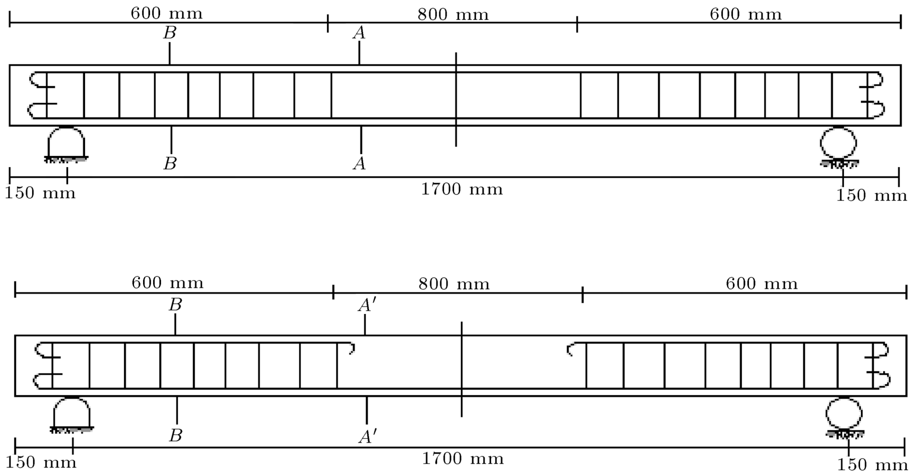

Figure 1a. Details of tested beam.

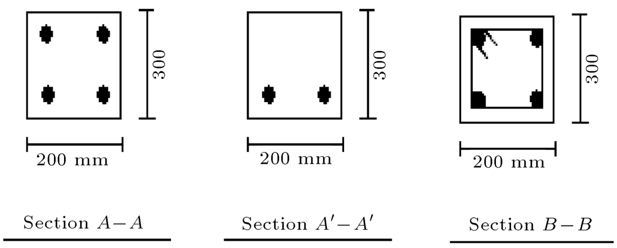

Figure 1b. Details of sections for tested beams.

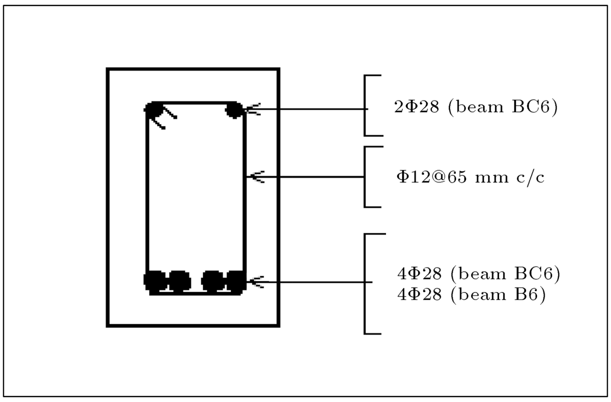

Figure 1c. Details of sections for beams B6 and BC6.

a) Singly under-reinforced beams (for beams B6 and B7):

$$\phi_y = \frac{f_y}{E_s d(1-K)}, \tag{1}$$

$$K = -\rho n + [2\rho n + \rho^2 n^2]^{1/2}, \tag{2}$$

$$\phi_u = \frac{\varepsilon_{cu}}{X_u}, \tag{3}$$

$$X_u = \frac{\rho f_y d}{\alpha\beta_1 f'_c}, \tag{4}$$

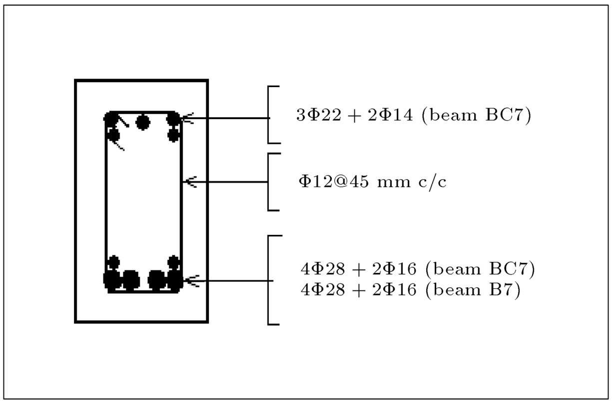

Figure 1d. Details of sections for beams B7 and BC7.

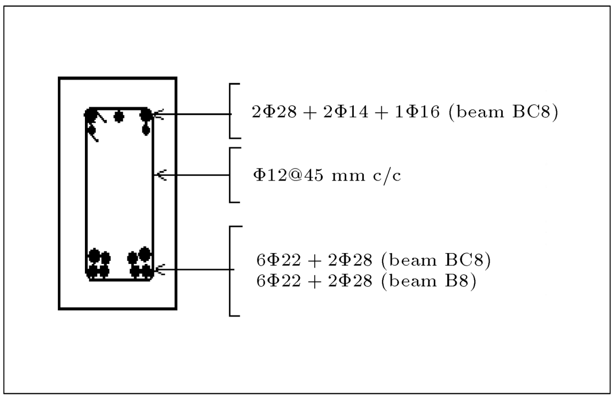

Figure 1e. Details of sections for beams B8 and BC8.

$$\mu_\phi = \frac{\phi_u}{\phi_y} = \frac{\varepsilon_{cu}(\alpha\beta_1 f'_c)E_s(1+\rho n(2\rho n+\rho^2 n^2)^{1/2})}{\rho f_y^2}. \tag{5}$$

And for singly over-reinforced beams (for beam B8), ultimate curvature is:

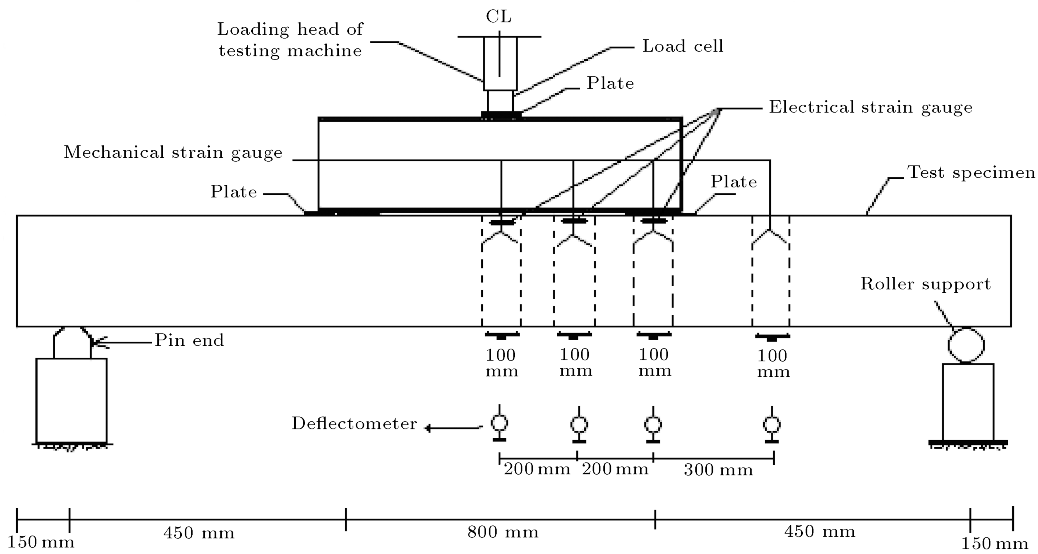

Figure 1f. Testing arrangement.

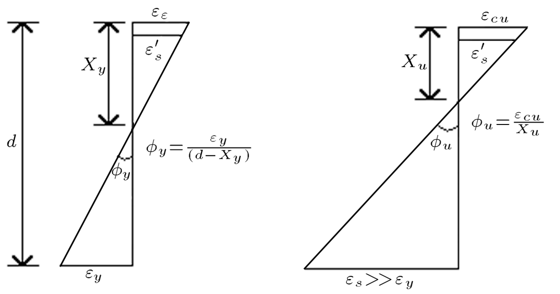

Figure 2. Strain diagrams at yield and ultimate loads.

$$\phi_u = \frac{\varepsilon_{cu}}{X_u}, \tag{6}$$

$$X_u^2 + \left(\frac{\varepsilon_{cu}\rho d}{\alpha\beta_1 f_c'}\right) X_u - \left(\frac{\varepsilon_{cu}\rho d^2}{\alpha\beta_1 f_c'}\right) = 0. \tag{7}$$

b) Doubly under-reinforced beams:

$$\phi_y = \frac{f_y}{E_s d(1-K)},$$

and:

$$\phi_u = \frac{\varepsilon_{cu}}{X_u},$$

$$K = \left[n^2(\rho+\rho')^2 + 2n\left(\rho + \frac{\rho' d'}{d}\right)^2\right]^{1/2} - n(\rho+\rho'), \tag{8}$$

where compression reinforced is yield (for beam BC8):

$$\phi_u = \varepsilon_{cu}\frac{\alpha\beta_1 f_c' b}{(A_s - A_s')f_y}, \tag{9}$$

$$\mu = \frac{\alpha\beta_1 f_c' \varepsilon_{cu} E_s}{f_y^2(\rho - \rho)}(1-K), \tag{10}$$

where compression reinforced is not yield (for beams BC6 and BC7):

$$X_u = \left[\frac{(\rho' E_s\varepsilon_{cu} - \rho f_y)^2 d^2}{(2\alpha f_c')^2\beta_1^2} + \frac{\rho' E_s \varepsilon_{cu} d d'}{(\alpha f_c')\beta_1}\right]^{1/2} - \frac{(\rho' E_s\varepsilon_{cu} - \rho f_y)d}{(2\alpha f_c')\beta_1}, \tag{11}$$

$$\mu_\phi = \frac{\phi_u}{\phi_y} = \frac{E_s\varepsilon_{cu}(1-K)d}{f_y X_u}, \tag{12}$$

where:

X_u = neutral axis at ultimate state,
X_y = neutral axis at yielding state,
α = the stress block coefficient,
β_1 = the ratio between the height of the stress block and X_u,
E_s = modulus of elasticity of steel.

Based on ACI and CSA codes for normal strength concret [9,10], theoretical calculations for the curvature ductility of HSC were performed and the results are shown in Table 3.

Displacement Ductility

Displacement ductility is defined as the ratio of deflection at the ultimate load to the deflection at the first yielding of the tensile steel. Ultimate load is the maximum load applied for a beam during testing.

The deflection of a beam can be derived from curvature. According to the curvature-area theorem:

$$\Delta_m = \int X\varphi dX. \tag{13}$$

Table 3. Theoretical curvature ductility of tested beams.

Beam No.	Theoretical (ACI)			Theoretical (CSA)		
	$\phi_y \times 10^{-5}$ (1/mm)	$\phi_u \times 10^{-5}$ (1/mm)	μ_ϕ	$\phi_y \times 10^{-5}$ (1/mm)	$\phi_u \times 10^{-5}$ (1/mm)	μ_ϕ
BC6	1.41	3.89	2.75	1.41	4.95	3.51
B6	1.58	2.36	1.49	1.58	2.94	1.86
BC7	1.44	2.99	2.07	1.44	3.82	2.65
B7	1.65	2.20	1.33	1.65	2.74	1.66
BC8	1.58	2.78	1.76	1.58	3.45	2.18
B8	a	1.86	-	a	2.10	-

a: The B8 is an over-reinforced beam, (i.e., $\varepsilon_{sf} < \varepsilon_y$).

Considering the idealized curvature for a two-point load of tested beams, as shown in Figure 3 [1], one can get:

$$\Delta_{y,m} = \phi_y \frac{z_1^2}{3} + \phi_y z_2 \left(z_1 + \frac{z_2}{2}\right), \tag{14}$$

$$\Delta_{u,m} = \phi_y \frac{z_1^2}{3} + (\phi_u - \phi_y) L_p \left(z_1 - \frac{L_p}{2}\right) + \phi_u z_2 \left(z_1 + \frac{z_2}{2}\right), \tag{15}$$

$$\mu_\Delta = \frac{\Delta_{u,m}}{\Delta_{y,m}}, \tag{16}$$

where:

Δ_{ym}, φ_y = displacement and curvature at mid-span, respectively, when the longitudinal tension reinforcement yields;
Δ_{um}, φ_u = displacement and curvature at mid-span, respectively, when the compression concrete is crushed;
Z_1 = shear span;
Z_2 = distance between mid-span and concentrated load;
L_p = plastic length, which can be estimated as follows [2]:

$$L_p = 0.08 Z_1 + 0.022 d_b f_y \text{ (MPa)}, \tag{17}$$

where d_b is the diameter of longitudinal tension reinforcement.

Based on ACI and CSA codes, theoretical calculations for displacement ductility were performed and the results are shown in Table 4.

Rotation Ductility

The rotation of the region at the midspan was calculated by multiplying average curvature by the length at which that curvature is valid, i.e. equal to effective depth, d [6]. The average curvature was determined from the strain variation along the height of the beam.

Based on ACI and CSA codes, theoretical calculations for the rotation ductility of the beams were performed and the results are shown in Table 5.

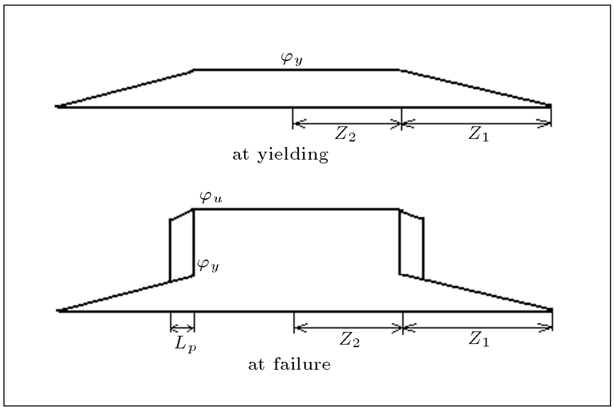

Figure 3. Idealized curvature of simply supported beam.

Rotation Ductility in Total Beam Length

A measure of total rotation in the yield and ultimate state for the whole length of the span was obtained in the same manner as that shown in Figure 4 [11,12]. For simplicity, it is assumed that the plastic hinge is concentrated at the midspan.

Based on Figure 4, rotation at yield and ultimate states (θ_y, θ_u) are, respectively, equal to:

$$\theta_y = 2\text{arctag}2\frac{\delta_y}{l}, \tag{18}$$

$$\theta_u = 2\text{arctag}2\frac{\delta_u}{l}, \tag{19}$$

where δ_y is the deflection at the onset of the reinforcement yielding, δ_u is the deflection at ultimate load and l is the length of the beam span.

Table 4. Theoretical deflection ductility of tested beams.

	Theoretical (ACI)			Theoretical (CSA)		
Beam No.	Δ_y (mm)	Δ_u (mm)	$\mu_d = \Delta_u/\Delta_y$	Δ_y (mm)	Δ_u (mm)	$\mu_d = \Delta_u/\Delta_y$
BC6	4.61	13.23	2.87	4.61	16.91	3.67
B6	5.17	7.88	1.52	5.17	9.89	1.91
BC7	4.71	10.09	2.14	4.71	12.98	2.75
B7	5.40	7.33	1.35	5.40	9.22	1.70
BC8	5.17	9.34	1.80	5.17	11.66	2.25
B8	a	-	-	a	-	-

a: The B8 is an over-reinforced beam (i.e., $\varepsilon_{sf} < \varepsilon_y$).

Table 5. Theoretical rotation ductility of tested beams.

	Theoretical (ACI)			Theoretical (CSA)		
Beam No.	θ_y (rad)	θ_u (rad)	μ_θ	θ_y (rad)	θ_u (rad)	μ_θ
BC6	0.0036	0.0099	2.75	0.0036	0.0126	3.51
B6	0.0040	0.0060	1.49	0.0040	0.0075	1.86
BC7	0.0038	0.0079	2.07	0.0038	0.0101	2.65
B7	0.0043	0.0058	1.33	0.0043	0.0073	1.69
BC8	0.0040	0.0071	1.76	0.0040	0.0089	2.18
B8	a	0.0048	-	a	0.0054	-

a: The B8 is an over-reinforced beam (i.e., $\varepsilon_{sf} < \varepsilon_y$).

Based on ACI and CSA codes and by using Equations 18 and 19, theoretical calculations for the rotation ductility in the total length of the span were performed and the results are summarized in Table 6.

EXPERIMENTAL RESULT

Curvature Ductility

For the tested beams, the experimental values of the curvature under yield and ultimate conditions and also their curvature ductility are reported in Table 7. The experimental curvature values are determined on the basis of the mechanical strain gauges (demec points) measured for concrete and electrical strain gauges mounted on tensile reinforcement for any load increment (see Table 7).

Where ε_{cc} and ε_{cu} are the measured extreme compressive concrete strain at yielding of the tensile steel and beam failure, respectively, and ε_y and ε_{sf} are measured as tensile steel strains at yielding and beam failure, respectively.

From the test results, it is possible to plot the moment-curvature diagram up to beam failure. The

Table 6. Theoretical rotation ductility for total span length of tested beams.

	Theoretical (ACI)			Theoretical (CSA)		
Beam No.	θ_y (rad)	θ_u (rad)	μ_θ	θ_y (rad)	θ_u (rad)	μ_θ
BC6	0.0108	0.0311	2.88	0.0108	0.0317	3.67
B6	0.0121	0.0185	1.52	0.0121	0.0232	1.92
BC7	0.0111	0.0237	2.14	0.0111	0.0305	2.76
B7	0.0127	0.0172	1.36	0.0127	0.0217	1.70
BC8	0.0121	0.0219	1.81	0.0121	0.0274	2.26
B8	a	-	-	a	-	-

a: The B8 is an over-reinforced beam (i.e., $\varepsilon_{sf} < \varepsilon_y$).

Table 7. Experimental measurements and curvature ductility of tested beams.

Beam No.	$\phi_y \times 10^{-5}$ (1/mm)	$\phi_u \times 10^{-5}$ (1/mm)	$\mu_\phi = \phi_u/\phi_y$	ε_y	ε_{cc}	ε_{sf}	ε_{cu}
BC6	1.44	6.24	4.33	0.0018	0.0023	0.0125	0.0034
B6	2.35	2.55	1.08	0.0018	0.00390	0.0019	0.0041
BC7	1.73	[a]	-	0.0021	0.0019	0.0056[b]	0.0025 [b]
B7	1.26	2.25	1.77	0.0020	0.0015	0.0030	0.0027
BC8	1.50	5.07	3.38	0.0021	0.0016	0.0109	0.0036
B8	1.77	2.48	1.40	0.0018	0.0027	0.0026	0.0038

a: The electrical strain gauge was disconnected.

b: The last reading taken before the gauge is disconnected.

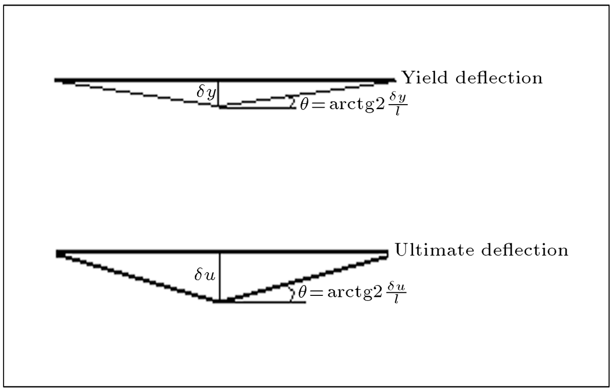

Figure 4. Relationship of total rotation to mid-span deflection.

moment-curvature curves at the mid-span section of tested beams are shown in Figure 5.

Displacement Ductility

Based on the experimental deflections at yielding of tensile reinforcement, Δ_y, and ultimate load, Δ_u, shown in Table 8, the load-deflection curves are plotted and shown in Figure 6.

Rotation Ductility

For the tested beams, the experimental rotation values at yield and ultimate conditions and, also, their rotation ductility are reported in Table 9. The moment-rotation curves at the mid-span section are shown in Figure 7.

Table 8. Experimental deflection ductility of tested beams.

Beam No.	Δ_y (mm)	Δ_u (mm)	$\mu_d = \Delta_u/\Delta_y$
BC6	8.88	19.70	2.22
B6	9.28	9.70	1.04
BC7	13.53	25.67	1.89
B7	6.95	12.84	1.84
BC8	10.40	16.73	1.61
B8	8.76	14.00	1.59

Table 9. Experimental rotation ductility of tested beams.

Beam No.	θ_y	θ_u	μ_θ
BC6	0.0037	0.0159	4.34
B6	0.0060	0.0065	1.08
BC7	0.0044	-	-
B7	0.0032	0.0057	1.79
BC8	0.0038	0.0129	3.38
B8	0.0045	0.0063	1.40

Rotation Ductility in Total Beam Length

Considering Figure 4, the experimental rotation at yield and ultimate loads (θ_y, θ_u) and the rotation ductility for the whole length of the span are calculated and the results are presented in Table 10.

COMPARISON BETWEEN DIFFERENT TYPES OF DUCTILITY

For two codes studied, the different types of theoretical and experimental ductility are compared and the results are shown in Figures 8-10.

Table 10. Experimental rotation ductility for whole span length of beams.

Beam No.	θ_y	θ_u	μ_θ
BC6	0.0096	0.0213	2.22
B6	0.0100	0.0105	1.04
BC7	0.0146	0.0277	1.89
B7	0.0075	0.0139	1.85
BC8	0.0112	0.0181	1.61
B8	0.0095	0.0151	1.59

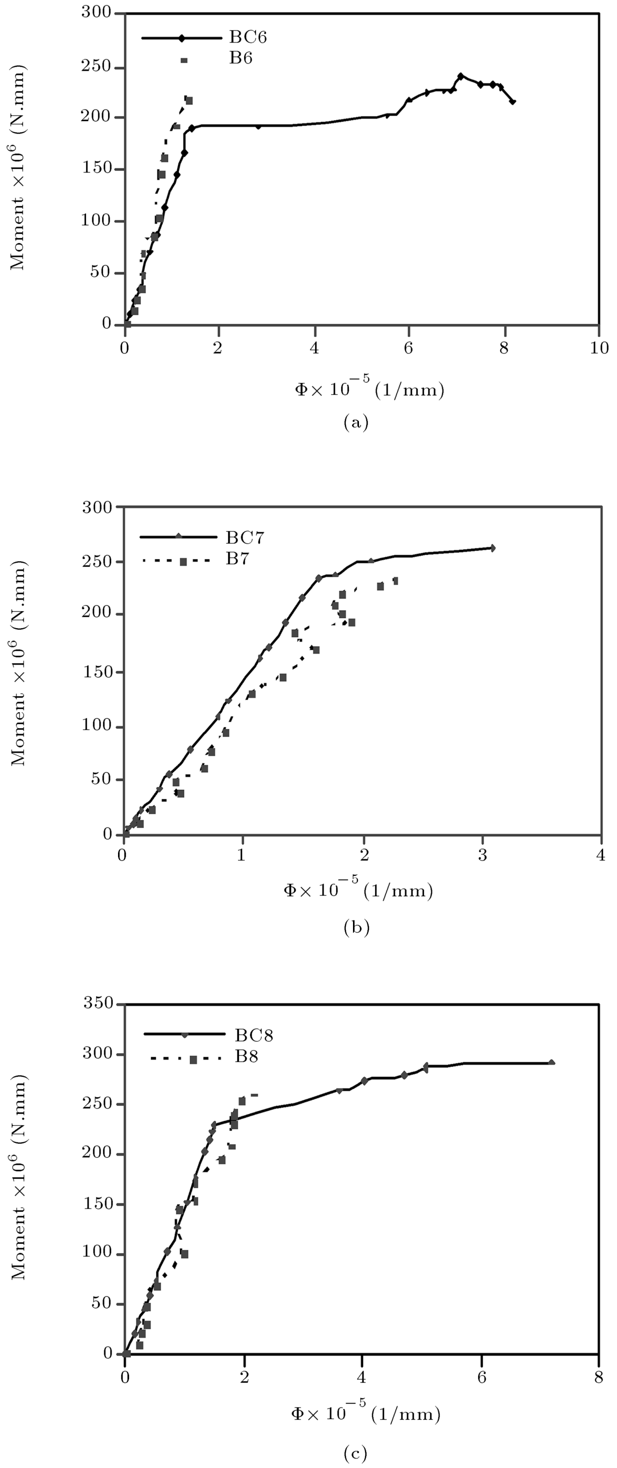

Figure 5. Moment-curvature curves of tested beams.

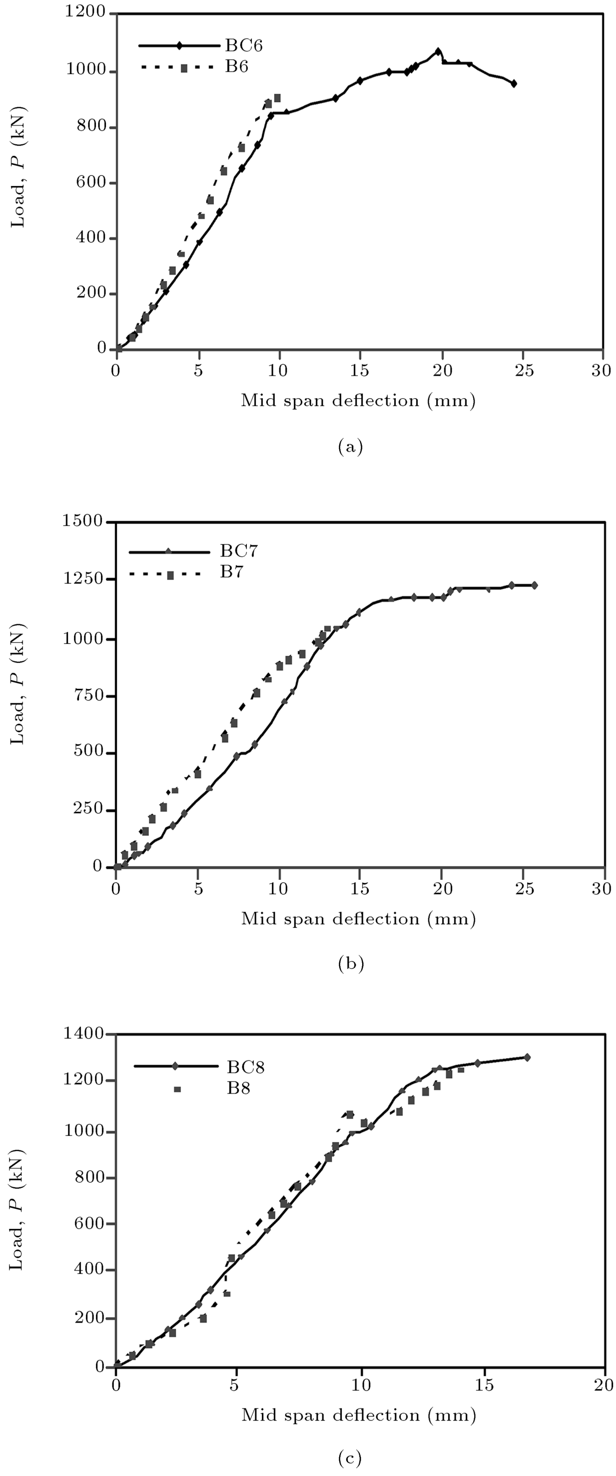

Figure 6. Load-deflection curves of tested beams.

MODE OF FAILURE

The beams are loaded step by step and crack propagations and the failure mode for some tested beams are shown in Figures 11-13. Refering to the experimental measurement results of Table 7 and Figures 11-13, it is clear that for heavily reinforced HSC tested beams (without any stirrup in the constant moment region), the mode of failure occured in the tension manner (i.e., the first tensile rebar reached yield and then the concrete reached a value for ε_{cu} greater than 0.003 (suggested by the ACI code expected by beam B7)). However, the ductility is not good enough to use this type of beam in seismic regions.

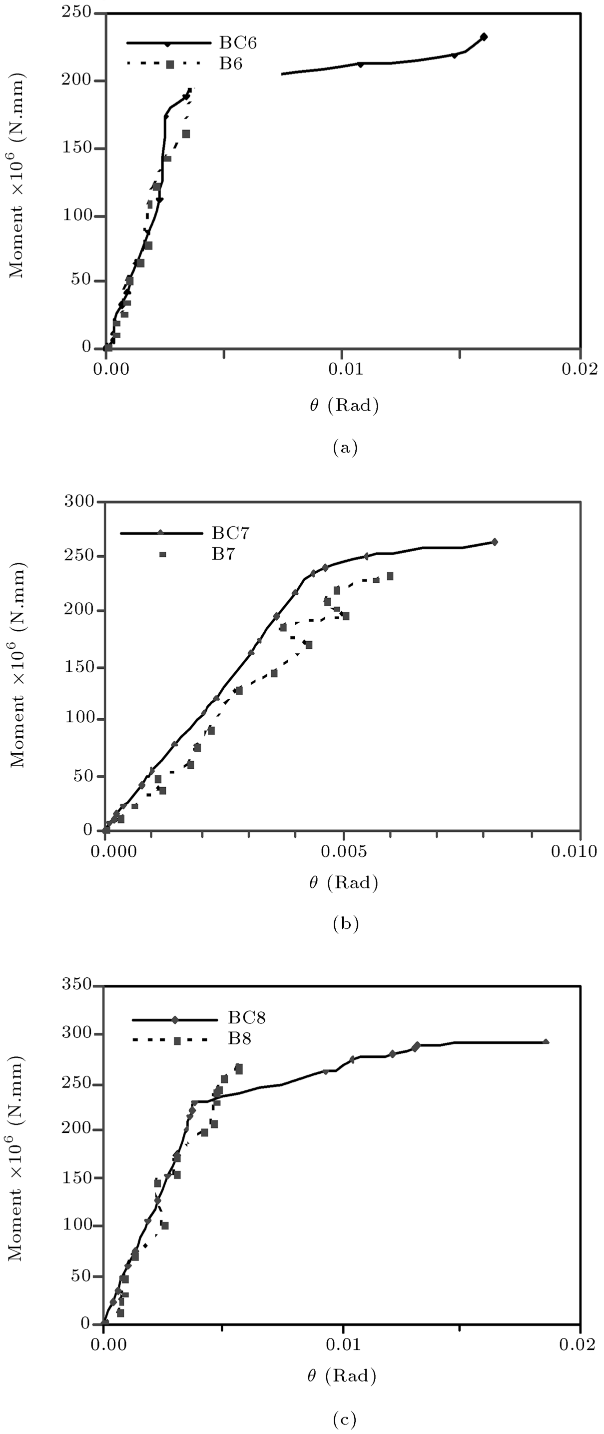

Figure 7. Moment rotation curves of tested beams.

COMPARISON OF DIFFERENT TYPES OF EXPERIMENTAL DUCTILITY

The comparison of two different types of experimental ductility (curvature and displacement ductilities) was performed and the results are presented in Table 11. It is clear that for singly HSC heavily steel reinforced beams, the curvature ductility is too close to the displacement ductility.

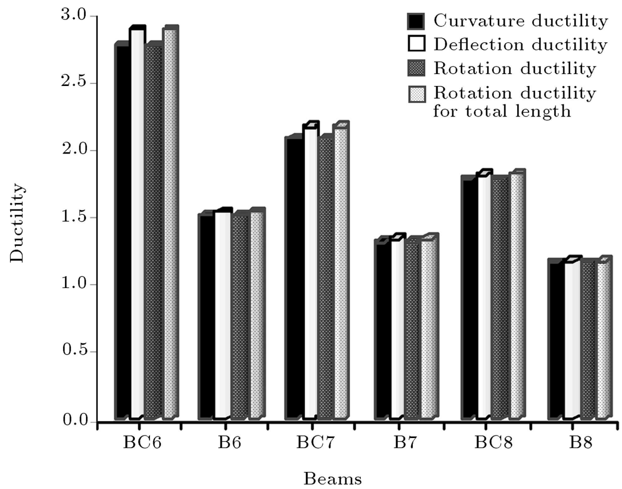

Figure 8. Comparison of different types of theoretical ductility based on ACI code.

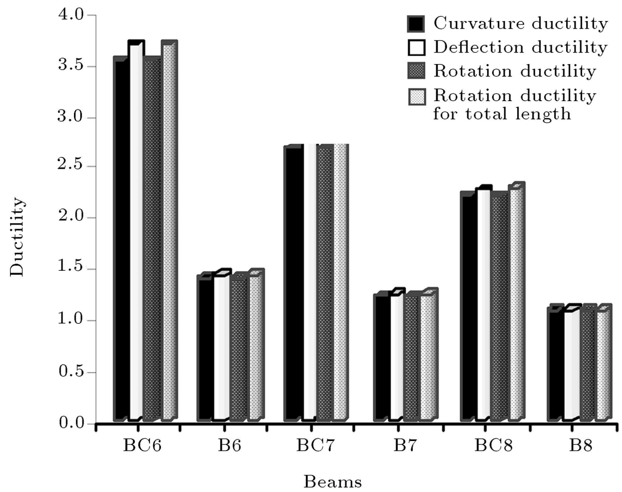

Figure 9. Comparison of different types of theoretical ductility based on CSA code.

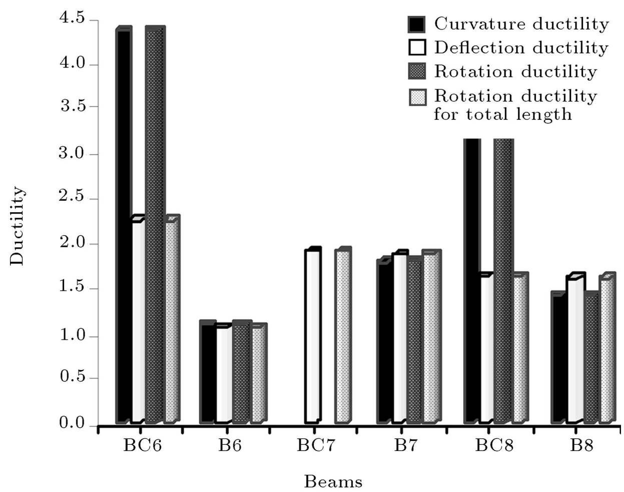

Figure 10. Comparison of different types of experimental ductility.

Figure 11. Crack propagation of beams under load.

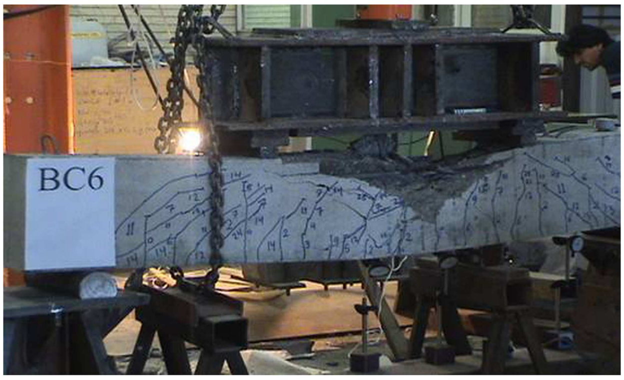

Figure 12. Collapse of beam BC6 under load.

Figure 13. Crack propagation of beam BC7 under load.

CONCLUSION

For heavily steel reinforced HSC beams tested in flexure, the following conclusions can be drawn:

1. The theoretical displacement ductility is too close to the theoretical curvature ductility;
2. The exprimental displacement ductility is lower than the theoretical displacement ductility;
3. The theoretical displacement and curvature in the yield state for doubly reinforced beams are lower than the singly reinforced beams;

Table 11. Comparison of different types of experimental ductility.

Beam No.	μ_d	μ_ϕ
BC6	2.22	4.33
B6	1.04	1.08
BC7	1.89	-
B7	1.84	1.77
BC8	1.61	3.38
B8	1.59	1.40

4. By adding half a percentage of ρ as compressive steel, the ultimate displacement, curvature and rotation were increased;
5. For the singly HSC reinforced beams, the difference between the experimental curvature and displacement ductility values is relatively low, but for doubly HSC reinforced tested beams, the experimental curvature ductility is higher than the experimental displacement ductility;
6. The theoretical ductility values suggested by CSA and ACI methods are very close, but the experimental values of the curvature ductility are higher than the theoretical values. However, this is more obvious for doubly HSC reinforced beams;
7. As expected, the rotation ductilities (rotation ductility in a section and in total beam length) of those obtained from curvatures and deflections are similar to the curvature and displacement ductilities, respectively.

REFERENCES

1. Tsong, Y., Yue, L.H. and Jaw, W.T. "Amelioration of stirrup and compression reinforcement on the ductility of reinforced high strength concrete beam", in *Proceeding of the Sessions Related to Seismic Engineering and Structures Congress*, San Francisco, CA., pp. 596-604 (1989).
2. Pauly, T. "Seismic design of reinforced concrete structures", in *2nd International Conference on Seismology and Earthquake Engineering*, Tehran, Iran, pp. 1-20 (1995).
3. Maghsoudi, A.A., *Design for Ductility of Structures*, Shahid Bahonar University Publications, Kerman, Iran (1996).
4. Chien-Hung, L. and Feng-Sheng, L. "Ductility of high-performance concrete beams with high-strength lateral reinforcement", *ACI Structural Journal*, **98**(4), pp. 600-608 (2001).
5. Park, R. and Dai, R. "Ductility of doubly reinforced concrete beam sections", *ACI Structural Journal*, **85**(85), pp. 217-225 (1989).
6. Ricardo, N.F. do carmo and Sergio, M.R. lopes "Ductility and linear analysis with moment redistribution

in reinforced high-strength concrete beams", *Can. J. Civ. Eng.*, **32**, pp. 194-203 (2005).

7. Sharifi, R.Y. "Effect of tensile and compressive over reinforcement ratio on ductility and behavior of high-strength concrete flexural members", MSc. Thesis, Department of Civil Engineering, University of Kerman, Iran (2005).

8. Mohammad Hasani, M. "Ductility of reinforcement high-strength concrete beams with high longitudinal tensile reinforcement ratio (special for seismic areas)", MSc. Thesis, Department of Civil Engineering, University of Kerman, Iran (2004).

9. ACI Committee 318 "Building code requirement for structural concrete (ACI 318-05) and commentary (318R-05)", American Concrete Institute, Farmington Hills, Mich. (2005).

10. CSA 94, CSA Technical Committee "Design of concrete structure for buildings", CAN3-A23.3-M94, Canadian Standards Association, Rexdale, Ontario (1994).

11. Mattock, A.H. "Rotational capacity of hinging regions in reinforced concrete beams", in *Proceeding of the International Symposium on Flexural Mechanics of Reinforced Concrete*, SP-12, American Concrete Institute, Farmington Hills, Mich., pp. 143-181 (1964).

12. Corley, W.G. "Rotational capacity of reinforced concrete beams", *Journal of Structural Division, ASCE*, ST5, **92**, pp. 121-146 (1966).